

Article

Multi-Objective Distributionally Robust Optimization for Earthquake Shelter Planning Under Demand Uncertainties

Kai Tang * and Toshihiro Osaragi 

Department of Architecture and Building Engineering, School of Environment and Society, Institute of Science Tokyo, Tokyo 152-8550, Japan; osaragi.t.20f7@m.isct.ac.jp

* Correspondence: tang.k.ac@m.titech.ac.jp; Tel.: +81-09049014130

Abstract: Deciding the locations of shelters and how to assign evacuees to these locations is crucial for effective disaster management. However, the inherent uncertainty in evacuation demand makes it challenging to make optimal decisions. Traditional stochastic or robust optimization models tend to be either too aggressive or overly conservative, failing to strike a balance between risk reduction and cost. In response to these challenges, this research proposes a multi-objective distributionally robust optimization (MODRO) model tailored for shelter location and evacuation allocation. First, an ambiguity set (moment-based or distance-based) is constructed to capture the uncertainty in evacuation demand, reflecting the possible range of outcomes based on demand data from a disaster simulation model. Then, the distributionally robust optimization model considers the “worst-case” distribution within this ambiguity set to minimize construction cost, travel distance, and unmet demand/unused capacity, balancing the trade-off between overly conservative and overly optimistic approaches. The model aims to ensure that shelters are optimally located and evacuees are efficiently allocated, even under the most challenging scenarios. Furthermore, Pareto optimal solutions are obtained using the augmented ϵ -constraint method. Finally, a case study of Ogu, a wooden density built-up area in Tokyo, Japan, compares the DRO model with stochastic and robust optimization models, demonstrating that the cost obtained by the DRO model is higher than a stochastic model while lower than the worst-case robust model, indicating a more balanced approach to managing uncertainty. This research provides a practical and effective framework for improving disaster preparedness and response, contributing to the resilience and safety of urban populations in earthquake-prone areas.

Keywords: shelter; earthquake; distributionally robust optimization; moment-based ambiguity set; Wasserstein distance



Citation: Tang, K.; Osaragi, T. Multi-Objective Distributionally Robust Optimization for Earthquake Shelter Planning Under Demand Uncertainties. *GeoHazards* **2024**, *5*, 1308–1325. <https://doi.org/10.3390/geohazards5040062>

Academic Editor: Hans-Balder Havenith

Received: 13 November 2024

Revised: 10 December 2024

Accepted: 11 December 2024

Published: 16 December 2024



Copyright: © 2024 by the authors. Licensee MDPI, Basel, Switzerland. This article is an open access article distributed under the terms and conditions of the Creative Commons Attribution (CC BY) license (<https://creativecommons.org/licenses/by/4.0/>).

1. Introduction

The number of reported disasters has increased over the past two decades [1]. The increasing frequency and intensity of natural disasters have increasingly emphasized the urgent need for reasonable disaster management. This surge has also highlighted the necessity of comprehensive strategies that span mitigation, preparedness, response, and recovery. Each of these phases is critical in reducing disaster risks and managing their impacts effectively. Emergency humanitarian logistics, which plays an essential role in mobilizing and delivering critical resources to affected populations in limited time, is a big challenge for effective disaster management. One of the key logistical components in disaster management is the optimal location planning of humanitarian facilities such as shelters, warehouses, and healthcare centers, which collectively form the backbone of relief operations. Shelter location planning, in particular, is vital across all disaster management phases. In the mitigation phase, strategically located shelters can reduce potential loss of life and property. During the preparedness phase, having well-distributed shelters ensures communities are ready to respond to anticipated risks. In the response phase, shelters' proximity to impacted areas facilitates rapid and efficient relief efforts, as they

are essential for providing immediate protection to evacuees. Lastly, during the recovery phase, shelters offer temporary housing and support services that enable communities to begin rebuilding and returning to normalcy. This critical role of shelter location planning in disaster management has led to a significant body of research focusing on optimization models for shelter locations.

The shelters are designed for earthquakes, floods, hurricanes, and other disasters. Earthquakes are a major hazard that frequently happen in Japan. In history, big earthquakes have resulted in massive casualties. It is forecasted that a major earthquake will strike in Tokyo in the near future [2]. Except Japan, other areas also face the threat of an earthquake. In 2023, the Kahramanmaraş earthquake that hit Turkey and Syria killed more than 53,000 people and forced 2 million people to become evacuees. To reduce the possible losing of life and property, it is necessary to make sure that all people can arrive at shelters as soon as possible. In Tokyo Metropolitan, the government usually appoints elementary schools, middle schools, and other public buildings as official shelters. According to the disaster mitigation plan, these shelters are able to accept most people in need under usual emergency conditions. However, if the previously mentioned major earthquake happens, existing shelters cannot accept all evacuees as before due to the increased scale of the disaster and the resulting surge in evacuation demand. The task is to select the optimal locations from many potential locations and decide the adequate capacity for each selected shelter. The main challenge lies in uncertain demand, which means that the number of residents who are in need of shelters is unknown before making decisions. The most common way is by applying the stochastic programming that assumes that the probability distribution of uncertain demand is known. Another challenge is to handle the relationship between efficiency and cost. In order to deal with it, multi-objective optimization models that set distance or construction cost as the objectives were proposed in past research. However, it is hard to obtain the true probability distribution of uncertain demands, and unlike the emergency logistics optimization problem [3,4], in which transportation costs for delivering relief supplies and construction costs can be directly combined into a single monetary objective, the shelter location allocation problem involves the transportation of people. In this context, distances cannot be easily quantified in monetary terms and thus cannot be directly aggregated with the construction or operational costs from the first stage.

Therefore, to deal with these difficulties, in this study, instead of a single objective or single stage model, we propose a multi-objective distributionally robust optimization (MODRO) model aiming to aid decision-making by minimizing the mean value under the worst probability distribution from a set of possible distributions. The MODRO model considers three objectives: minimizing the total construction and operational costs, reducing the overall evacuation distance, and minimizing the number of unutilized shelter capacities, as well as the number of evacuees left without shelter. By adopting a multi-objective formulation, a pareto solution set can be obtained, and we anticipate that the distributionally robust optimization approach will enable authorities to make more informed and balanced decisions regarding the optimal location of shelters.

2. Literature Review

This part will review the literature on (i) the shelter location allocation problem and (ii) distributionally robust optimization.

2.1. Shelter Location Allocation Model

The shelter location allocation problem has been extensively studied in disaster management literature, with earthquakes [5–8], hurricanes [9–11], and floods [12–14] being the most addressed disaster types. Authors from different areas are concerned about different disasters. For example, researchers in North America care more about hurricanes [9,11,15] or other meteorological disasters like tornadoes [16,17]. Studies in earthquake-prone regions, like Italy and Turkey, focus more on earthquakes [8,18]. Disaster management is typically divided into two-phases: pre-disaster (preparedness) and post-disaster (re-

response). In the pre-disaster stage, the decision variables are usually location, capacity, or pre-positioned relief supplies, with the objective of minimizing the fixed or variable construction costs of new facilities and the costs of pre-positioned items. In the post-disaster stage, the decision variables include evacuation flow, unmet demand, relief flow, shortage, and unused relief supplies. The goal of this phase is to minimize the transportation cost, penalty cost for unmet demand, and shortage and surplus supplies. In the second stage, there are uncertainty parameters, making solving the problem a challenge. Among the different types of uncertainties (supply uncertainty, demand uncertainty, and network connectivity uncertainty), demand uncertainty is frequently addressed, which a large body of the literature focused on [11,19,20]. Stochastic programming (SP) is the most common approach to handling uncertainties in such problems. When the probability distribution of random parameter is known or assumed to follow a specific distribution, SP can be applied to minimize the expected value of the second stage objective function under the predefined probability distribution. However, it is not easy to know the “true probability distribution” of demand or other uncertain parameters; therefore, many studies have adopted the SAA (sample average approximation) [21–23] to deal with this problem. However, SAA requires a large number of samples to accurately represent uncertainty, which can significantly increase computational costs and complexity. Additionally, SAA solutions may suffer from high variability if the sample size is insufficient. There is another problem for using the two-stage SP to solve the shelter location allocation problem: there are few studies that have dealt with the shelter location allocation problem for earthquake evacuation. Earthquake evacuation is different from hurricane evacuation or the relief distribution problem, which usually needs to travel for a long distance using a car. For earthquake evacuation, it is important to ensure evacuees can quickly walk to a safe place in a short time due to fire spreading; therefore, the objective in the response stage should be the total travel distance instead of traveling cost. This will make the traditional two-stage stochastic programming model unsuitable to solve such a problem, since distance cannot be added together with construction cost.

2.2. Distributionally Robust Optimization

As we will describe in Section 3, distributionally robust optimization is the main method we will use in this study, so, in this part, we will perform a review on it. Stochastic programming (SP) is commonly used in the research of humanitarian facility locations [4], as we described in Section 2.1; however, it is hard to meet the requirements of SP, since there are usually limited historical data. Therefore, recently, more and more studies have adopted robust optimization (RO) to ensure the system works well even if in the worst situation [24–27]. Therefore, as one type of RO, distributionally robust optimization (DRO) can be seen as a mixture of SAA and worst-case RO. This is because SAA assumes that the probability of each realization of uncertain parameter is the same; instead, worst-case RO only considers the worst realization while setting the probabilities of other realizations as 0. However, DRO tries to obtain the optimal value under the worst probability distribution. Therefore, it can be anticipated that the objective value obtained by DRO will be between the SAA and worst-case RO. These results have been verified by [27,28]. DRO realizes this effect by constructing an ambiguity set that contains those probability distributions that meet certain criteria, thus providing a more conservative and robust approach to decision-making under uncertainty. The set that contains all these possible probability distributions is called the ambiguity set, which is the key component in a DRO model that encapsulates the uncertainty in the probability distribution governing the problem. The ambiguity set is built based on certain information, including support and moment information [29,30], “distance” from the reference distribution [31,32], and the structural properties [33,34]. Typically, for the moment-based ambiguity set, the range of mean and variance will be defined, while the distance-based ambiguity set contains the distributions that are close to a reference distribution. The DRO can be transformed into a semidefinite programming (SDP) problem, which can be efficiently solved using the cutting surface

method [35,36] or dual method [30,33,37]. Compared to SP and RO, DRO offers greater flexibility in constructing the uncertainty set; also, in practical applications, the solution of DRO is resilient, with lower costs, which makes it suitable to solve problems in disaster management. However, the research on earthquake evacuation seems to have not benefited from the development of DRO. Therefore, this research aims to (i) propose a multi-objective distributionally robust optimization model to solve earthquake shelter location allocation planning and (ii) use an alternating gradient descent ascent (PDHG) method to solve scenario-based DRO problems.

3. Model Formulation

It is necessary to consider not only construction/maintenance costs in the preparedness phase but also the travel distance and surplus/deficit of shelter capacity in the response stage. Therefore, we adopt a two-stage model formulation, as described in Figure 1. However, because the units are different, these objective functions cannot be directly summed together, as is commonly done in many two-stage stochastic optimization models for the disaster management problem [3]. Therefore, we adopt a three-objective formulation that contains all these objectives. The objectives of distance and capacity surplus/deficit are estimated for the response phase in disasters, which is called the second-stage objective in a two-stage formulation. In this research, we use a scenario-based DRO to formulate these two objective functions.

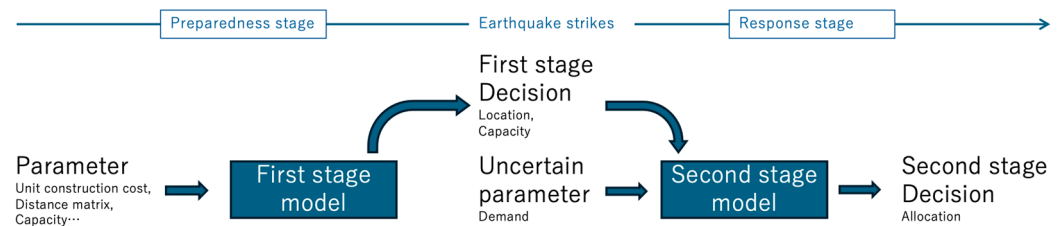


Figure 1. Two-stage model.

3.1. Formulation of the Ambiguity Set

In this research, we adopt two widely used approaches: a moment-based set and Wasserstein distance-based set.

3.1.1. Moment-Based Ambiguity Set

The moment-based ambiguity set is a commonly used set that usually regulates the range of the first moment (expected value) and second moment (variance), and its general form is

$$U = \left\{ \mathbb{P} \in \mathbb{R}^N \mid v^- \leq \mathbb{E}_{\mathbb{P}} \left[\left(\xi - \bar{\xi} \right) \left(\xi - \bar{\xi} \right)^T \right] \leq v^+ \right\}, \tag{1}$$

where ξ is the uncertain parameter, and $\bar{\xi}$ is the mean of ξ , which can be estimated from partial data. The set U contains a distribution \mathbb{P} , which makes the expected value ($\mathbb{E}_{\mathbb{P}}[\xi]$) and variance ($\mathbb{E}_{\mathbb{P}} \left[\left(\xi - \bar{\xi} \right) \left(\xi - \bar{\xi} \right)^T \right]$) of ξ within a certain range. In order to obtain a robust solution that is effective even in the worst conditions, it is required to choose the “worst probability”, which maximizes the value of the objective function. Consider that we have a convex problem with the following form:

$$\min_x f(x, \xi), \tag{2}$$

s.t.

$$x \in X, \tag{3}$$

in which ξ is an uncertain parameter vector about which we only know partial information, $f(x, \xi)$ is the convex function, and X is a convex set. Therefore, the DRO form of the original problem can be written as

$$\min_x \max_{\mathbb{P}_\xi} f(x, \xi), \tag{4}$$

s.t.

$$x \in X, \tag{5}$$

$$\mathbb{P}_\xi \in U, \tag{6}$$

For the discrete problem, which means that there are finite realizations of ξ , the inner problem of Equation (4) can be written as

$$\max \sum_i p_i f(x, \xi_i), \tag{7}$$

s.t.

$$\sum_i p_i = 1, \tag{8}$$

$$\sum_i p_i \xi_i = u, \tag{9}$$

$$v^- \leq \sum_i p_i \left[(\xi_i - \bar{\xi}) (\xi_i - \bar{\xi})^T \right] \leq v^+, \tag{10}$$

in which p_i is the probability of scenario i , and ξ_i is the realization of ξ in scenario i . It is obvious that, for finite scenarios, this problem turns out to be linear programming (LP).

3.1.2. Wasserstein Distance-Based Ambiguity Set

A distance-based ambiguity set is a collection of probability distributions that are defined based on a specific measure of distance between the distributions. In the context of the DRO, this set includes all distributions within a certain distance from a reference distribution, typically measured using a specific metric. One common choice is the Wasserstein distance, which quantifies the minimum cost of transporting probability mass to transform one distribution into another. The Wasserstein ambiguity set thus encompasses all distributions within a specified Wasserstein distance from the empirical or nominal distribution, allowing for robust solutions that account for distributional uncertainty within this defined range. The general form of a Wasserstein distance-based ambiguity set is

$$U = \{ \mathbb{P} \in \mathbb{R}^N : W(\mathbb{P}, \mathbb{Q}) \leq \delta \}, \tag{11}$$

in which $W(\mathbb{P}, \mathbb{Q})$ is the Wasserstein distance between probability distribution \mathbb{P} and reference distribution \mathbb{Q} , and δ is a threshold or radius that controls how “close” the distributions within the ambiguity set must be to \mathbb{Q} .

For discrete problems, the set can be rewritten as the following optimization problem:

$$\min_{\pi} \sum_i \sum_j \pi_{ij} s_{ij}, \tag{12}$$

s.t.

$$\sum_i \pi_{ij} = q_j \quad j = 1, \dots, M, \tag{13}$$

$$\sum_j \pi_{ij} = p_i \quad i = 1, \dots, N, \tag{14}$$

in which s_{ij} is the “distance” between the reference probability distribution \mathbb{Q} and obtained probability distribution \mathbb{P} . p_i is the probability of scenario i for the obtained probability distribution \mathbb{P} , and q_j is the probability of scenario j for the reference probability distribution \mathbb{Q} . π_{ij} is the transportation plan, representing how much probability mass should be moved from point i in distribution \mathbb{P} to point j in distribution \mathbb{Q} .

3.1.3. Estimation of the Mean and Variance

For both moment-based and distance-based sets, an estimated mean and variance are necessary. In this part, we will introduce how to use an earthquake simulation model [30] to estimate the mean and variance of the uncertain parameter, which is the demand vector in our problem, and we denote it as $\mathbf{d} = \{d_1, \dots, d_k\}$. We define the demand as “number of people in each demand point who are in need of staying in shelters due to house damage or other situations”. By this definition, we can be obtained by the following steps: (i) determine the population in each building by assuming that the population distribution is proportional to the building’s floor area; assign attributes to each building, where the structure type is predefined and the building age is randomly generated; (ii) for buildings with different attributes (age and structure), compute the complete collapse rate of each building based on the parameters of normal distribution in Table 1 (λ and ζ are the mean and standard deviation of the building fragility curves; from the curve, we can obtain the collapse rate of certain building types under different PGVs (peak ground velocities; it refers to the maximum speed at which the ground moves during an earthquake, used to assess seismic intensity and potential structural damage); these parameters are estimated from the historical data of Kumamoto earthquake; (iii) randomly determine the state of each building (collapse or not) based on the probability we obtained by step (ii). By following these three steps, the demand of a single scenario can be acquired. Repeat the process n times, and n demand samples can be generated. The estimated mean and variance then can be acquired by (15) and (16). The reference distribution used by the distance-based set can be regarded as the uniform distribution with the estimated mean.

$$\bar{\mathbf{d}} = \frac{1}{n} \sum_i d_i, \tag{15}$$

$$\Sigma = \frac{1}{n} \sum_i (d_i - \bar{d}_i) (d_i - \bar{d}_i)^T, \tag{16}$$

Table 1. Parameters for various building types ¹.

Building Structure	Building Age	λ	ζ
Wooden	~1971	4.84	0.71
	1972~1981	5.11	0.76
	1982~1991	5.41	0.64
	1992~2001	5.70	0.70
	2002~	6.62	0.89
RC	~1971	5.12	0.65
	1972~1981	5.33	0.58
	1982~	6.00	0.79
Steel	~1971	4.64	0.62
	1972~1981	4.97	0.49
	1982~	5.64	0.73

¹ The parameters are estimated by the data from Kumamoto earthquake [38].

3.2. Formulation of Multi-Objective Distributionally Robust Optimization

In this study, we investigate a network that is composed of multiple shelters and demand points during two time periods: before and after disasters occur. Evacuees relocate from the demand point to the shelter after disaster occurs, and the emergency supplies kept in shelters should meet the uncertain demands from demand points. There are two decisions being made in the network: in the stage before disaster, the decision maker makes decision on the locations and capacities of shelters from multiple potential locations, decision makers can refer to the model’s results to determine where to build shelters and their appropriate scale. Meanwhile, in the stage after a disaster, the decision will be made on how many evacuees should be allocated to the shelters selected in the first stage. These

decisions correspond to specific scenarios, enabling decision makers to use these results as a reference for making personnel allocation decisions in similar situations. We consider the demand as a random parameter that refers to the number of people in need of relocating to shelters, and this parameter is highly uncertain, because only people who lose their houses will become evacuees, and the state of the house damage is uncertain due to the uncertain nature of the disaster. The objectives of this model include the objective of the before disaster stage: minimization of the expenses needed to establish all selected shelters and the objectives of the after disaster stage: minimization of the total evacuation distance and minimization of unmet demands and unused capacity. The unmet demands are measured by the number of unallocated people who are in need of being transferred to shelters due to house damage. The unused capacities are measured by the number of additional evacuees the shelters can accommodate using the remaining supplies after all persons have taken shelter. The notations of the model are summarized in Table 2, and the details of the objectives are shown in Table 3.

Table 2. Notations of the parameters, variables, and sets.

Category	Name	Description
Parameter (scalar)	f_i	Fixed cost for shelter i , measured by Japanese yen.
	v	Variable cost (unit cost corresponding to one evacuee), measured by Japanese yen.
	t_{ki}	Shortest travel distance from demand point k to shelter i , measured by meter.
	$d_k(s)$	Demand at demand point k at scenario s , measured by number of people.
	M	A big number.
	I	Number of potential shelters.
	K	Number of demand points.
Decision variable (scalar)	x_i	1 if potential shelter i is selected, 0 otherwise.
	c_i	Capacity of shelter i , measured by number of people.
	$q_{ki}(s)$	Number of people allocated from demand point k to selected open shelter i at scenario s .
	p_s	Probability of scenario s .
Set	U	Ambiguity set.

Table 3. Details of the objectives.

Stage	Objective Type	Objective Detail	Measurement
First stage: before-disaster	Establish cost data	Fixed cost	$\sum_{i \in I} f_i x_i$
		Variable cost	$\sum_{i \in I} c_i v$
Second stage: after-disaster	Shortage and surplus	Total evacuation distance	$\sum_{k \in K} \sum_{i \in I} t_{ki} q_{ki}(s)$
		Unmet demand	$\sum_{k \in K} \left(d_k(s) - \sum_{i \in I} q_{ki}(s) \right)$
		Unused capacity	$\sum_{i \in I} \left(c_i - \sum_{k \in K} q_{ki}(s) \right)$

We propose a two-stage multi-objective DRO (MODRO) to solve this location allocation problem. The formulations of the three objectives are as follows:

$$f_1 = \min_{x,c} (\sum_{i \in I} f_i x_i + \sum_{i \in I} c_i v), \tag{17}$$

$$f_2 = \min_q \max_p \sum_{s \in S} p_s [\sum_{k \in K} \sum_{i \in I} t_{ki} q_{ki}(s)], \tag{18}$$

$$f_3 = \min_{q,c} \max_p \sum_{s \in S} p_s [\sum_{k \in K} (d_k(s) - \sum_{i \in I} q_{ki}(s)) + \sum_{i \in I} (c_i - \sum_{k \in K} q_{ki}(s))], \tag{19}$$

As it is shown in Table 3, f_1 is a first stage objective function consisting of fixed cost and variable cost, in which $\sum_{i \in I} f_i x_i$ sums up the fixed cost for selected shelters, and $\sum_{i \in I} c_i v$ calculates the cost that corresponds to the number of evacuees. Fixed cost means the cost for each selected shelter, while variable cost refers to the cost for each evacuee. The details of these two types of cost for our case can be seen in Section 5.1. f_2 is a second stage objective function that can be regarded as the expected value of the total evacuation distance for all scenarios. It sums up the distance from one demand point to the assigned shelter of all evacuees who walk between them. f_3 is a second stage objective function that can be seen as the expected value of the sum of the unmet demand and unused capacity, in which $\sum_{k \in K} (d_k(s) - \sum_{i \in I} q_{ki}(s))$ measures the number of people who had not been allocated to shelters for all K demand points, and $\sum_{i \in I} (c_i - \sum_{k \in K} q_{ki}(s))$ measures the amount of capacities that are above the number of evacuees for all I shelters. f_2 and f_3 are formulated as DRO forms, respectively. The variable p_s is the “worst” probability of scenario s . It means to choose one probability distribution from the moment set U that makes the expected value of the objectives for all the maximum scenarios, then optimize it under this distribution. The details of the moment set will be introduced in the next section. The constraints for the model are from Equations (20)–(25). Equation (20) ensures that the number of people at each demand point allocated to shelters will not exceed the number of people at this point. Equation (21) makes sure that the number of evacuees assigned to each shelter will not exceed the capacity limit. In Equation (22), M is a large positive constant, and it makes sure that, if the location is not selected ($x_i = 0$), then the capacity will also be 0. Equation (23) regulates that x_i is the binary variable. Equations (24) and (25) state that other decision variables should be non-negative.

$$\sum_{i \in I} q_{ki} \leq d_k \quad k = 1, \dots, K, \tag{20}$$

$$\sum_{i \in I} q_{ki} \leq c_i \quad i = 1, \dots, I, \tag{21}$$

$$Mx_i \geq c_i \quad i = 1, \dots, I, \tag{22}$$

$$x_i \in \{0, 1\}, \tag{23}$$

$$c_i \geq 0 \quad i = 1, \dots, I, \tag{24}$$

$$q_{ki} \geq 0 \quad i = 1, \dots, I, k = 1, \dots, K, \tag{25}$$

4. Solution Approach

The MODRO combines multi-objective optimization and distributionally robust optimization. It was solved by Wang, Song [32] using AUGMECON after reformulation as a multi-objective MILP. For that kind of problem, we need to first reformulate the DRO problem, then solve the multi-objective problem. In order to facilitate the reformulation,

we firstly rewrite the model into a compact form (the meaning and size of each vector and matrix can be seen in Table 4):

$$f_1 = \min_{x,c} [f^T x + v^T c], \tag{26}$$

$$f_2 = \minmax_q \mathbb{E}_{\mathbb{P}} [t^T q], \tag{27}$$

$$f_3 = \minmax_{c,q} \mathbb{E}_{\mathbb{P}} [\alpha^T c - \rho^T q + \theta^T d], \tag{28}$$

Table 4. Notations of the parameters and variables in vector or matrix form.

Category	Name	Size	Description
Parameter (scalar)	I	1	Number of potential shelters.
	K	1	Number of demand points.
	S	1	Number of scenarios.
Parameter (vector/matrix)	f	$I \times 1$	Vector of fixed cost.
	v	$I \times 1$	Vector of variable cost (all element is equal to v).
	t	$(KI) \times 1$	Vector of distance.
	α	$I \times 1$	All-one column vector.
	ρ	$I \times K$	All-two column vector.
	θ	$K \times 1$	All-one column vector.
	D	$K \times S$	Matrix of uncertain demand of K demand points in S scenarios.
Decision variable (vector/matrix)	x	$I \times 1$	Vector of location decision.
	c	$I \times 1$	Vector of capacity decision.
	Q	$S \times (KI)$	Matrix of evacuee flows in S scenarios.
	p	$S \times 1$	Discrete probability distribution of demand.

In which, α is the all-one column vector with length I , ρ is the all-two column vector with size $I \times K$, and θ is the all-one column vector with length K . Because we deal with scenario-based problems, the second-stage objective functions f_2 and f_3 can be written as the min–max forms as follows:

$$f_2 = \minmax_Q [t^T Qp], \tag{29}$$

$$f_3 = \minmax_{c,Q} [\alpha^T c - \rho^T Qp + \theta^T Dp], \tag{30}$$

In which p is a $S \times 1$ column vector of probabilities, D is a $K \times S$ matrix of the uncertain demand with all S scenarios, and Q is a $S \times KI$ matrix of evacuee flows with all scenarios.

$$D = \begin{bmatrix} d_1(1) & \cdots & d_1(S) \\ \vdots & \ddots & \vdots \\ d_K(1) & \cdots & d_K(S) \end{bmatrix}, \tag{31}$$

$$Q = \begin{bmatrix} q_{11}(1) & \cdots & q_{KI}(1) \\ \vdots & \ddots & \vdots \\ q_{K1}(S) & \cdots & q_{KI}(S) \end{bmatrix}, \tag{32}$$

Equations (29) and (30) are the standard min–max form; therefore, we have transformed the scenario-based DRO into a saddle point problem [39]. An example of a saddle point can be seen in Figure 2. To solve this problem, we use the primal–dual hybrid gradient (PDHG) method, which alternates between minimizing the objective with respect to one variable and maximizing with respect to another, using gradient updates in each step. The Figure 3 shows the steps for solving f_2 , similar for f_3 .

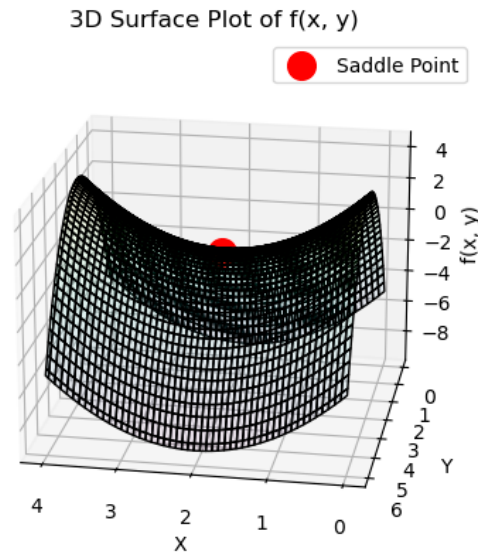


Figure 2. An example of a saddle point.

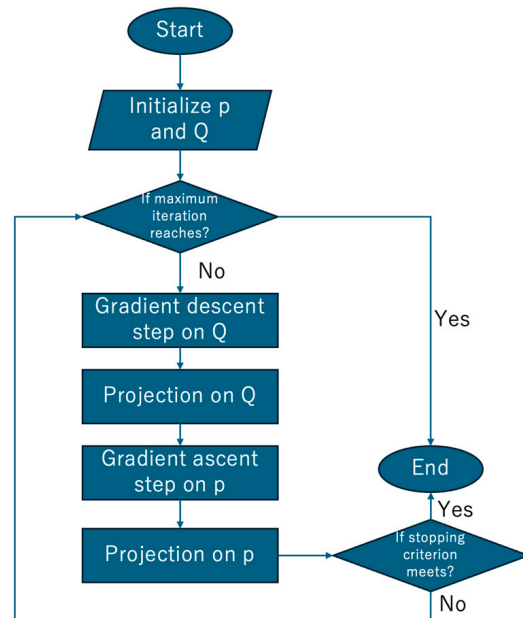


Figure 3. Flowchart of PDHG.

The projections for Q and p ensure that the variable after the descent/ascent step is still located in a feasible region. By minimization the distance between “new” and “old” locations, Projections (33)–(36) can obtain the “closest” location that meets the constraints for Q , and Projections (37) and (38) can acquire the “closest” distribution to that in ambiguity set U . U can be a distance-based set or moment-based set, and the details can be seen in Section 3.1. The product of two step sizes η_p and η_q (these two step sizes correspond to descent and ascent steps, respectively) should be less than 1 in order for convergence. In our problem, the order of magnitude of probability is far less than the number of people; we therefore set a small η_p with a big η_q .

$$\min_z \|z - Q^t\|^2, \tag{33}$$

s.t.

$$\sum_{i \in I} Q_{ki}^t(s) \leq d_k(s) \quad k = 1, \dots, K, s = 1, \dots, S, \tag{34}$$

$$\sum_{k \in K} Q_{ki}^t(s) \leq c_i \quad i = 1, \dots, I, s = 1, \dots, S, \tag{35}$$

$$Q_{ki}^t(s) \geq 0 \quad k = 1, \dots, K, i = 1, \dots, I, s = 1, \dots, S \tag{36}$$

$$\min_z \|z - p^t\|^2, \tag{37}$$

$$p^t \in U, \tag{38}$$

The second part is to solve the multi-objective optimization. The modified epsilon constraint method called AUGMECON by Mavrotas [40] is used to solve it. The detailed steps are as follows: (i) construct a payoff table. Our main purpose is to obtain the optimal location and capacity of the shelters; therefore, we prioritize minimizing f_1 as our main optimization goal. Using the payoff table shown in Table 5, we can determine the lower bounds and range for f_2 and f_3 . For example, the lower bound for f_2 is the minimum values among all the optimization results for f_1 , the upper bound is the maximum value, and the range is the gap between the upper bound and the lower bound. These optimization models are solved using the commercial solver Gurobi (downloaded from <https://www.gurobi.com/downloads/> (accessed on 1 October 2024)).

Table 5. Details of the payoff table.

R11: Independently optimization result for f_1	R21: Optimization result for f_2 by setting $f_1 = R11$	R31: Optimization result for f_3 by setting $f_1 = R11$ and $f_2 = R21$
R12: Optimization result for f_1 by setting $f_2 = R22$	R22: Independently optimization result for f_2	R32: Optimization result for f_3 by setting $f_2 = R22$ and $f_1 = R12$
R13: Optimization result for f_1 by setting $f_3 = R33$	R23: Optimization result for f_2 by setting $f_3 = R33$ and $f_1 = R13$	R33: Independently optimization result for f_3

(ii) Solve the epsilon constraint problem to obtain Pareto solutions. The objective function and constraints of the epsilon constraint problem are shown by Equations (39)–(43), where lb_2 is the lower bound for f_2 , lb_3 is the lower bound for f_3 , k_2 and k_3 are the ranges for f_2 and f_3 , respectively, and g_2 and g_3 are the number of grid points (they indicate the number of solutions that can be acquired). i_2 and i_3 are integers; by changing i_2 from 1 to g_2 and i_3 from 1 to g_3 , we can obtain one solution for each pair of i_2 and i_3 . For each solution acquired, no other solution is considered superior without compromising at least one objective.

$$\min f_1, \tag{39}$$

s.t.

$$f_2 \leq e_2, \tag{40}$$

$$f_3 \leq e_3, \tag{41}$$

$$e_2 = lb_2 + \frac{i_2 k_2}{g_2}, \tag{42}$$

$$e_3 = lb_3 + \frac{i_3 k_3}{g_3} \tag{43}$$

(iii) Select the best solution from the Pareto set. Since we only need one solution, it is necessary to choose only one solution out from the Pareto sets obtained in the second step. Here, we use the ratio of unmet demand to unused capacity as the criteria to select the best solution; in other words, the solution with the value of the ratio closest to 1 will be selected.

5. Case Study and Results Analysis

5.1. Study Area and Data Preparation

The Ogu area, situated in the northeast of Tokyo Metropolitan, spans a total area of 2.7 km² with a population of 54,650 (as of November 2023). The location of this area is shown in Figure 4. The geology of this area is believed to consist of diluvial layers in the upland areas and alluvial layers in the lowland areas. This region is characterized by a large number of wooden structure buildings, rendering it vulnerable to both earthquakes and fires. According to the Ninth Community Earthquake Risk Assessment Study [41], approximately half of the communities in the Ogu area receive the highest risk ratings for both building collapse and fire hazards. The last major earthquake that happened in this region was the 1923 Great Kanto earthquake, which caused approximately 140,000 deaths and missing persons in the whole Kanto area. Regarding building damage, approximately 109,000 buildings were completely destroyed, and about 212,000 were completely burned down. Within this area, there are 34 demand points and 18 potential shelter locations (schools and other public buildings), which can be seen in Figure 5. Each demand point represents an administrative unit called Chōnaikai, comprising one or several communities. In Tokyo, the Chōnaikai is responsible for establishing and managing shelters, as well as stockpiling disaster relief supplies; therefore we choose it as the basic unit for allocation. In order to prepare for the possible major earthquake and the secondary earthquake, especially the fire spread, the Tokyo Metropolitan government has implemented a series of measures, including the construction of shelters. There are three types of shelters in Tokyo, which are temporary evacuation areas, evacuation area, and evacuation centers. The temporary evacuation areas consist of street parks, which are used for immediate evacuation right after earthquakes. The evacuation areas are large open spaces, like the university. It is fire-proof, which can protect evacuees from fire spread, which is very necessary, since Tokyo has many wooden buildings that are easily caught on fire. Finally, elementary schools and middle schools and other public buildings are appointed as evacuation centers, which can provide food and accommodations for evacuees. In this study, we discuss the evacuation centers.

Utilizing the methods proposed by Hirokawa and Osaragi [42], we obtained disaster simulation data, including the probabilities of building collapse, street blockage, and fire outbreak. It is important to note that the parameters used for estimating building collapse probabilities are derived from the research conducted after the 2016 Kumamoto earthquake and the 1995 Great Hanshin earthquake, as noted in Table 1, which are considered to be more accurate than previous studies. By employing the methods mentioned in Section 3.1.3, we can obtain the demand of different scenarios. As for the estimation of establishing cost, we classify the cost into fixed cost and variable cost. There is a standard of the amount of relief at each shelter in Tokyo, so we use the list of relief of Adachi (There is no description in Arakawa on the website.) and estimate the cost of relief at each shelter by the price on Amazon (<https://www.amazon.co.jp/> (accessed on 1 October 2024)) or Rakuten (<https://www.rakuten.co.jp/> (accessed on 1 October 2024)). Table 6 shows the values of these two parameters. The distance matrix between different nodes is estimated by the K-shortest algorithm using the network distance data. Shelter planning problem of this region is also studied by Tang and Osaragi [43].

Table 6. Classification of the cost.

Type	Item	Total Price (yen)
Variable cost	Rice, water, blanket, etc.	6010/person
Fixed cost	Generator, light, batteries, telephone, TV, etc.	4,690,979

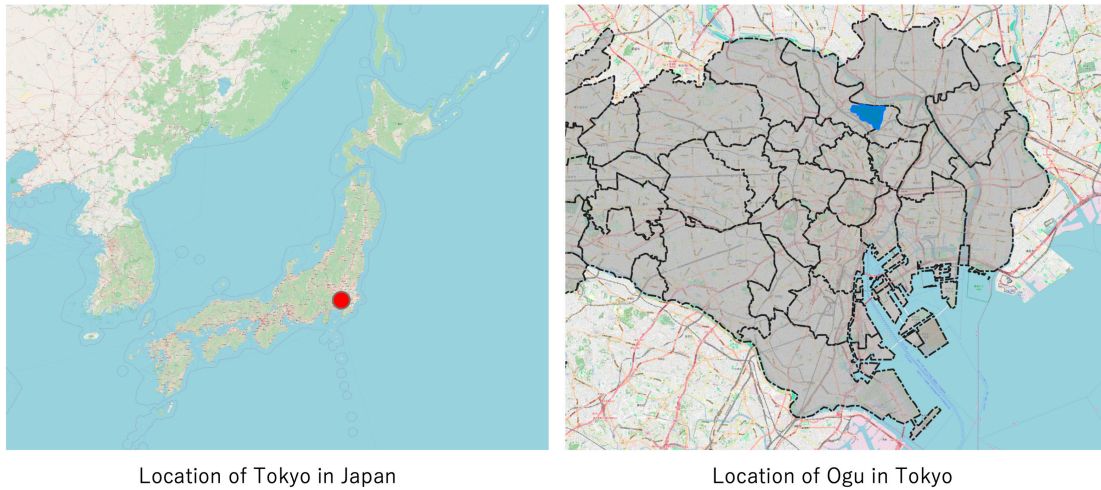


Figure 4. Location of the study area.

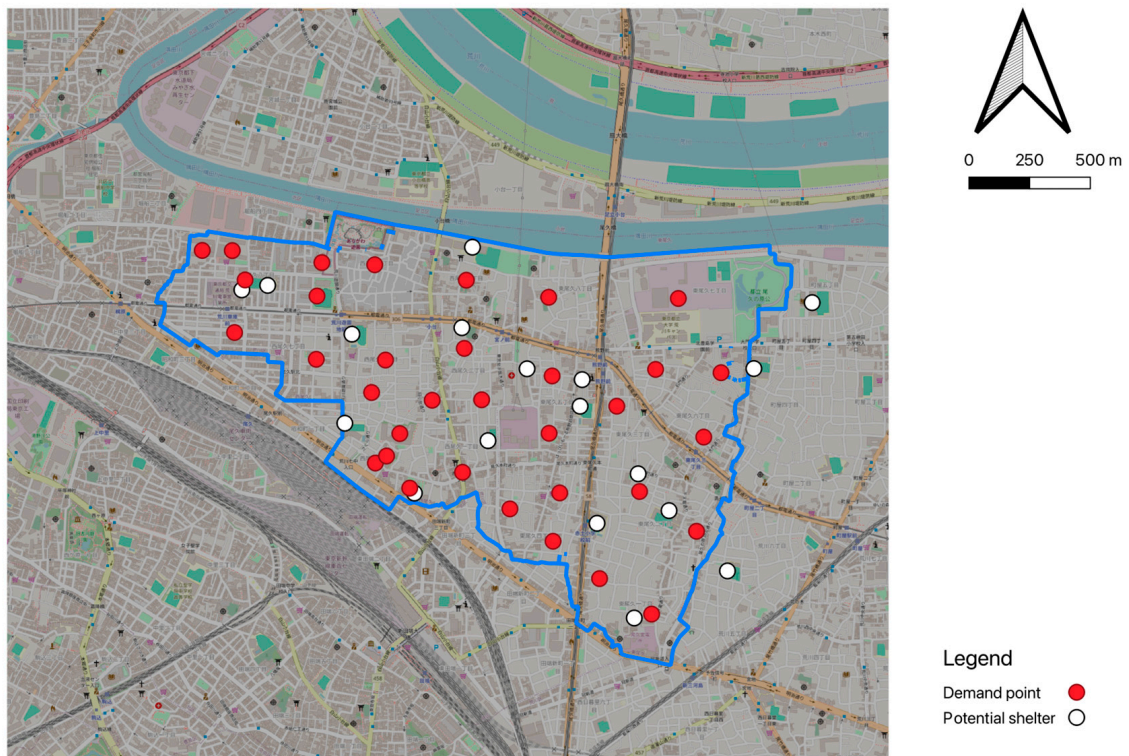


Figure 5. Demand points and potential shelters.

5.2. Performance of PDHG

The DRO model was implemented in Python 3.8 on a computer equipped with an Intel Core (8 cores, 2.3 GHz), 32 GB of DDR4 RAM. The toolbox used for solving the optimization problem is Gurobi. Since we hope to test the feasibility of applying this model in practice, we use the data described in Section 5.1 to test using the PDHG method to solve f3. From Table 7, we can see that, as the learning rate increases, the running time and required iteration are expected to decrease. *delta* is the parameter that regulates the size of the ambiguity set. As the size increases, the feasible region expands, and the running time also increases, since the computational difficulty generally increases with a larger feasible region. However, a larger ambiguity set means that there will be more probability distributions to choose, and it is more possible to generate a “better” solution finally.

Table 7. A summary of the CPU running time for solving f_3 using a distance-based ambiguity set.

δ	Step Size (η_p, η_q)	Iterations to Convergence	Running Time (s)
100	0.000001, 900,000	7	2411.24
	0.00005, 19,000	16	3629.54
	0.00001, 90,000	45	6789.12
500	0.000001, 900,000	10	3545.25
	0.00005, 19,000	17	4598.12
	0.00001, 90,000	67	8894.76

5.3. Sensitivity Analysis of the Ambiguity Set Size

Sensitivity analysis of the ambiguity set size is conducted. All the parameters except for the one under analysis are fixed. Since we want to see the impact on the DRO model, we test the influence of the parameter on the DRO solution for f_3 . A big size ambiguity set means that there will be more choice of probability distribution; however, it also means that it is possible to choose the probability distribution that is “far” away from the “true” distribution. Therefore, it is necessary to see the effect of enlarging the size of the ambiguity set. To verify the impact of the size of the ambiguity set on the DRO solution, we conducted a sensitivity analysis of the size of both the moment-based set and distance-based set. For the size of the distance-based set, we set the threshold δ range from 100 to 2000 and observed the value of f_3 . Figure 6 shows the impact of different δ on the value of f_3 : it can be seen that the value of f_3 increases as the size of the distance-based set increases; this is because there will be more choice for a “worse” distribution. After δ reaches around 1400, it will not change at all; this is because, when δ is big enough, we have already found the worst distribution. For the moment-based set, we set the r_1 from 0.2 to 1.0 and r_2 from 1.0 to 3.0. We can see from Figure 7 that the value of f_3 also increases with the enlargement of the ambiguity set, and after r_1 reaches around 0.8, it will never increase if r_2 remains the same. When fixed r_1 while r_2 increases, the value of f_3 will continue to increase until the maximum value is obtained. The maximum value is the same as the one obtained by the distance-based set. However, comparing these two sets, we can find that the distance-based set will show a broader range.

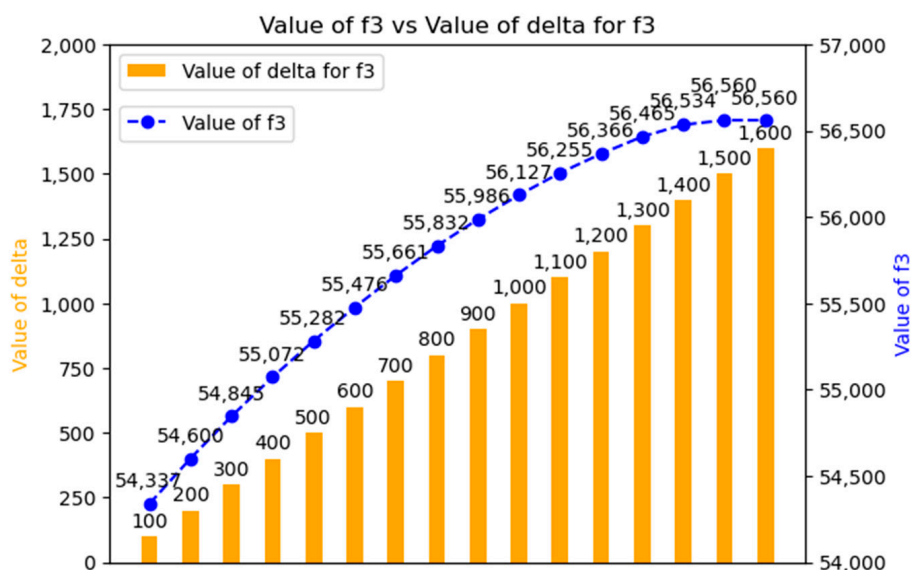


Figure 6. Sensitivity analysis of the size of the Wasserstein distance-based ambiguity set for f_3 .

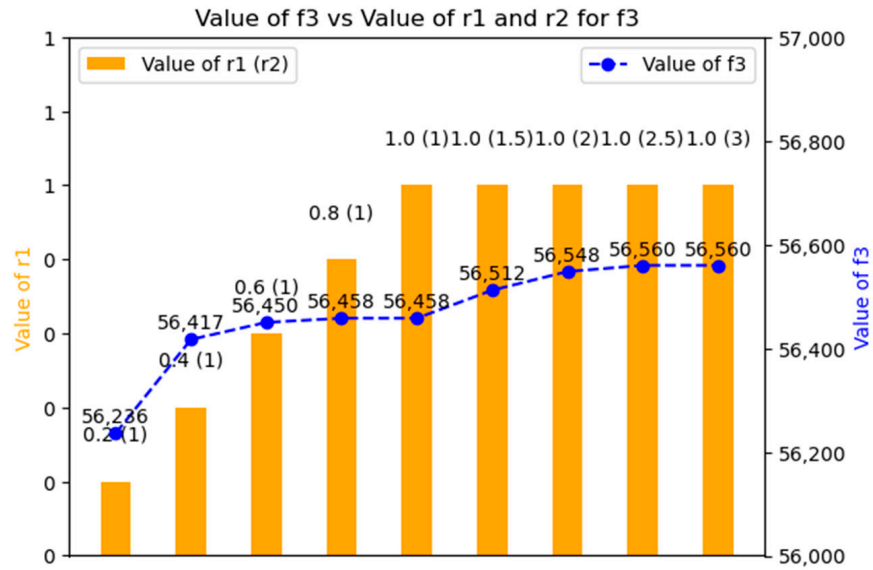


Figure 7. Sensitivity analysis of the size of the moment-based ambiguity set for f_3 .

5.4. Analysis of the DRO Solution

As shown in Section 5.3, when the size of the ambiguity set reaches a certain degree, the value of the optimization model will not change any more. We choose $r_1 = 0.6$ and $r_2 = 1.0$ to rule the size of the moment-based set and $\delta = 1200$ to regulate the size of the distance set. As described in Section 4, the Pareto solution can be obtained by AUGMECON, and we can obtain the best solution from the Pareto set. Figure 8 shows the selection of the best solution by the ratio of unmet demand to unused capacity. The red point is the solution with the ratio closest to 1.0. In addition, we also obtain the result of the SAA and worst-case RO to make a comparison. As expected, the results shown in Table 8 indicate that DRO can result in a solution that is better. The cost is between SAA and worst-case RO; however, the DRO showed better performance in allocating more evacuees to shelters than SAA.

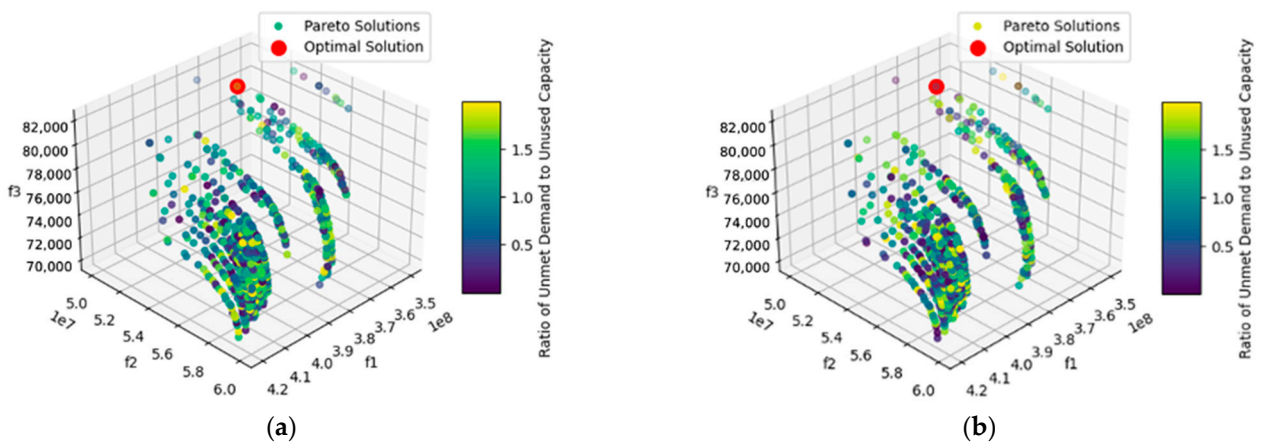


Figure 8. (a) Selection of the best solution from the Pareto set for MODRO ($r_1 = 0.6, r_2 = 1$). (b) Selection of the best solution from the Pareto set for MODRO ($\delta = 1200$).

Table 8. A comparison of the results by different models.

	Objective Value			Number of Selected Shelters
	f_1 (yen)	f_2 (m)	f_3 (People)	
MODRO ($r_1 = 0.6, r_2 = 1$)	369,509,830	50,913,964	81,124	16/18
MODRO ($\delta = 1200$)	360,990,800	50,685,047	80,900	16/18
SAA	352,921,119	59,973,533	100,975	15/18
worst-case RO	412,667,762	50,467,510	80,080	18/18

6. Discussion and Conclusions

The results obtained from the multi-objective distributionally robust optimization (MODRO) model for shelter location allocation planning under demand uncertainties demonstrate several findings. First, the comparison between the MODRO model and traditional stochastic and robust optimization models highlights the advantages of a distributionally robust approach. By considering the “worst-case” distribution within a moment-based or distance-based ambiguity set, the MODRO model effectively balances the trade-offs between cost, efficiency, and safety. This balance is crucial, as overly conservative models (worst-case RO) may result in unnecessarily high costs, while overly optimistic models (SAA) may fail to provide sufficient protection in the worst-case scenario. One key finding is that the construction cost under the MODRO model is consistently positioned between the costs derived from the worst-case RO and SAA. This indicates that the MODRO model provides a more balanced approach, neither too cautious nor too risky, thereby offering a more reliable framework for decision-making in disaster management. The MODRO model’s ability to incorporate uncertainty in a more nuanced manner allows for the identification of shelter locations that are not only cost-effective but also capable of accommodating evacuees under the most challenging scenarios.

Additionally, the model’s multi-objective nature allows for a more comprehensive analysis of the trade-offs between different goals. For instance, while the primary objective may be to minimize construction and operational costs, the model also considers the overall evacuation distance and the utilization rate of shelter capacities. This approach ensures that decisions are made not only with cost in mind but also with a focus on the overall efficiency and effectiveness of the evacuation process. The sensitivity analysis conducted as part of this study further underscores the robustness of the MODRO model. By adjusting the size of the ambiguity set, it becomes evident that the model can adapt to various levels of uncertainty. This flexibility is critical for real-world applications, where demand predictions are often imprecise, and the consequences of misallocation can be severe.

Although this study proposes a new approach to address this problem, several limitations must be acknowledged. First, due to the lack of sufficient historical data, we relied on simulation results. In reality, obtaining detailed, small-scale historical evacuation data is challenging. For example, for our study, the number of evacuees in each shelter under different scenarios is necessary, while it is not easy to acquire these data. Other data that need to be acquired are the building age data, which we currently cannot obtain in the study area. However, with advancements in remote sensing and other technologies, we hope that more real-world data will become accessible in the future. Further, the casualties will influence the demand, but we do not have enough data to estimate this. Second, it remains uncertain whether this method is applicable to areas beyond the current study region. Especially, the hierarchy of shelters are different in different areas, and many cities remain not only one type of area. Also, for some developed cities, it is unnecessary to discuss newly constructed shelters. Going forward, we aim to enhance the model’s applicability across a broader range of real-world scenarios. Third, the selection of the optimal solution from the Pareto solution set may be subjective, and the Pareto solution sometimes cannot ensure if a solution is reasonable. There are many standards to make the choice, and it is better to use the appropriate one according to different situations.

Author Contributions: Conceptualization, K.T. and T.O.; methodology, K.T. and T.O.; software, K.T.; validation, K.T.; formal analysis, K.T.; investigation, K.T.; resources, K.T.; data curation, K.T.; writing—original draft preparation, K.T.; writing—review and editing, K.T. and T.O.; visualization, K.T.; supervision, T.O. All authors have read and agreed to the published version of the manuscript.

Funding: This research received no external funding.

Data Availability Statement: The original contributions presented in this study are included in the article. Further inquiries can be directed to the corresponding author.

Conflicts of Interest: The authors declare no conflicts of interest.

References

1. UNDRR. *Annual Report 2022*; United Nations Office for Disaster Risk Reduction (UNDRR): Geneva, Switzerland, 2023.
2. Tokyo Metropolitan Government. *Report on Damage Estimates for Tokyo from a Directly Beneath the Capital Earthquake*; Bureau of Urban Development, Tokyo Metropolitan Government: Tokyo, Japan, 2022; p. 475.
3. Grass, E.; Fischer, K. Two-stage stochastic programming in disaster management: A literature survey. *Surv. Oper. Res. Manag. Sci.* **2016**, *21*, 85–100. [[CrossRef](#)]
4. Dönmez, Z.; Kara, B.Y.; Karsu, Ö.; Saldanha-Da-Gama, F. Humanitarian facility location under uncertainty: Critical review and future prospects. *Omega* **2021**, *102*, 102393. [[CrossRef](#)]
5. Döyen, A.; Aras, N.; Barbarosoğlu, G. A two-echelon stochastic facility location model for humanitarian relief logistics. *Optim. Lett.* **2011**, *6*, 1123–1145. [[CrossRef](#)]
6. Mete, H.O.; Zabinsky, Z.B. Stochastic optimization of medical supply location and distribution in disaster management. *Int. J. Prod. Econ.* **2010**, *126*, 76–84. [[CrossRef](#)]
7. Aghaie, S.; Karimi, B. Location-allocation-routing for emergency shelters based on geographical information system (ArcGIS) by NSGA-II (case study: Earthquake occurrence in Tehran (District-1)). *Socio-Econ. Plan. Sci.* **2022**, *84*, 101420. [[CrossRef](#)]
8. Kılçı, F.; Kara, B.Y.; Bozkaya, B. Locating temporary shelter areas after an earthquake: A case for Turkey. *Eur. J. Oper. Res.* **2015**, *243*, 323–332. [[CrossRef](#)]
9. Li, A.C.; Nozick, L.; Xu, N.; Davidson, R. Shelter location and transportation planning under hurricane conditions. *Transp. Res. Part E Logist. Transp. Rev.* **2012**, *48*, 715–729.
10. Rawls, C.G.; Turnquist, M.A. Pre-positioning of emergency supplies for disaster response. *Transp. Res. Part B Methodol.* **2010**, *44*, 521–534. [[CrossRef](#)]
11. Li, A.C.Y.; Xu, N.; Nozick, L.; Davidson, R. Bilevel Optimization for Integrated Shelter Location Analysis and Transportation Planning for Hurricane Events. *J. Infrastruct. Syst.* **2011**, *17*, 184–192. [[CrossRef](#)]
12. Mollah, A.K.; Sadhukhan, S.; Das, P.; Anis, Z. A cost optimization model and solutions for shelter allocation and relief distribution in flood scenario. *Int. J. Disaster Risk Reduct.* **2018**, *31*, 1187–1198. [[CrossRef](#)]
13. Lee, Y.-H.; Keum, H.-J.; Han, K.-Y.; Hong, W.-H. A hierarchical flood shelter location model for walking evacuation planning. *Environ. Hazards* **2020**, *20*, 432–455. [[CrossRef](#)]
14. Kongsomsaksakul, S.; Yang, C.; Chen, A. Shelter location-allocation model for flood evacuation planning. *J. East. Asia Soc. Transp. Stud.* **2005**, *6*, 4237–4252.
15. Sherali, H.D.; Carter, T.B.; Hobeika, A.G. A location-allocation model and algorithm for evacuation planning under hurricane/flood conditions. *Transp. Res. Part B Methodol.* **1991**, *25*, 439–452. [[CrossRef](#)]
16. Schmidlin, T.W.; Hammer, B.O.; Ono, Y.; King, P.S. Tornado shelter-seeking behavior and tornado shelter options among mobile home residents in the United States. *Nat. Hazards* **2008**, *48*, 191–201. [[CrossRef](#)]
17. Simmons, K.M.; Sutter, D. Direct estimation of the cost effectiveness of tornado shelters. *Risk Anal* **2006**, *26*, 945–954. [[CrossRef](#)]
18. Di Bucci, D.; Del Missier, F.; Dolce, M.; Galvagni, A.; Giordano, F.; Patacca, A.; Pezzi, E.; Scurci, G.; Savadori, L. Life satisfaction during temporary housing after an earthquake: Comparing three cases in Italy. *Int. J. Disaster Risk Reduct.* **2023**, *91*, 103697. [[CrossRef](#)]
19. Ozbay, E.; Çavuş, Ö.; Kara, B.Y. Shelter site location under multi-hazard scenarios. *Comput. Oper. Res.* **2019**, *106*, 102–118. [[CrossRef](#)]
20. Kulshrestha, A.; Wu, D.; Lou, Y.; Yin, Y. Robust Shelter Locations for Evacuation Planning with Demand Uncertainty. *J. Transp. Saf. Secur.* **2011**, *3*, 272–288. [[CrossRef](#)]
21. Alizadeh, M.; Amiri-Aref, M.; Mustafee, N.; Matilal, S. A robust stochastic Casualty Collection Points location problem. *Eur. J. Oper. Res.* **2019**, *279*, 965–983. [[CrossRef](#)]
22. Aslan, E.; Çelik, M. Pre-positioning of relief items under road/facility vulnerability with concurrent restoration and relief transportation. *IIE Trans.* **2019**, *51*, 847–868. [[CrossRef](#)]
23. Sanci, E.; Daskin, M.S. Integrating location and network restoration decisions in relief networks under uncertainty. *Eur. J. Oper. Res.* **2019**, *279*, 335–350. [[CrossRef](#)]
24. Zhang, P.; Liu, Y.; Yang, G.; Zhang, G. A distributionally robust optimisation model for last mile relief network under mixed transport. *Int. J. Prod. Res.* **2020**, *60*, 1316–1340. [[CrossRef](#)]

25. Zhang, P.; Liu, Y.; Yang, G.; Zhang, G. A distributionally robust optimization model for designing humanitarian relief network with resource reallocation. *Soft Comput.* **2020**, *24*, 2749–2767. [[CrossRef](#)]
26. Liu, K.; Li, Q.; Zhang, Z.-H. Distributionally robust optimization of an emergency medical service station location and sizing problem with joint chance constraints. *Transp. Res. Part B Methodol.* **2019**, *119*, 79–101. [[CrossRef](#)]
27. Wang, C.; Chen, S. A distributionally robust optimization for blood supply network considering disasters. *Transp. Res. Part E: Logist. Transp. Rev.* **2020**, *134*, 101840. [[CrossRef](#)]
28. Zhang, G.; Jia, N.; Zhu, N.; He, L.; Adulyasak, Y. Humanitarian transportation network design via two-stage distributionally robust optimization. *Transp. Res. Part B Methodol.* **2023**, *176*, 102805. [[CrossRef](#)]
29. Xu, H.; Liu, Y.; Sun, H. Distributionally robust optimization with matrix moment constraints: Lagrange duality and cutting plane methods. *Math. Program.* **2018**, *169*, 489–529. [[CrossRef](#)]
30. Delage, E.; Ye, Y. Distributionally Robust Optimization Under Moment Uncertainty with Application to Data-Driven Problems. *Oper. Res.* **2010**, *58*, 595–612. [[CrossRef](#)]
31. Del Barrio, E.; Giné, E.; Matrán, C. Central Limit Theorems for the Wasserstein Distance Between the Empirical and the True Distributions. *Ann. Probab.* **1999**, *27*, 1009–1071. [[CrossRef](#)]
32. Jiang, R.; Guan, Y. Data-driven chance constrained stochastic program. *Math. Program.* **2016**, *158*, 291–327. [[CrossRef](#)]
33. Hanasusanto, G.A.; Roitch, V.; Kuhn, D.; Wiesemann, W. A distributionally robust perspective on uncertainty quantification and chance constrained programming. *Math. Program.* **2015**, *151*, 35–62. [[CrossRef](#)]
34. Van Parys, B.P.G.; Goulart, P.J.; Morari, M. Distributionally robust expectation inequalities for structured distributions. *Math. Program.* **2017**, *173*, 251–280. [[CrossRef](#)]
35. Bansal, M.; Huang, K.-L.; Mehrotra, S. Decomposition Algorithms for Two-Stage Distributionally Robust Mixed Binary Programs. *SIAM J. Optim.* **2018**, *28*, 2360–2383. [[CrossRef](#)]
36. Rahimian, H.; Mehrotra, S. Frameworks and Results in Distributionally Robust Optimization. *Open J. Math. Optim.* **2022**, *3*, 4. [[CrossRef](#)]
37. Bertsimas, D.; Sim, M.; Zhang, M. Adaptive Distributionally Robust Optimization. *Manag. Sci.* **2019**, *65*, 604–618. [[CrossRef](#)]
38. Torisawa, K.; Matsuoka, M.; Horie, K.; Inoguchi, M.; Yamazaki, F. Building Fragility Curves Based on Disaster-Victim Certificate Data of Multiple Local Governments Covering a Wide Range of Seismic Motion in the 2016 Kumamoto Earthquake. *J. Jpn. Assoc. Earthq. Eng.* **2021**, *21*, 5_98–5_118. [[CrossRef](#)]
39. Liu, Y.; Yuan, X.; Zeng, S.; Zhang, J. Primal–dual hybrid gradient method for distributionally robust optimization problems. *Oper. Res. Lett.* **2017**, *45*, 625–630. [[CrossRef](#)]
40. Mavrotas, G. Effective implementation of the ϵ -constraint method in Multi-Objective Mathematical Programming problems. *Appl. Math. Comput.* **2009**, *213*, 455–465. [[CrossRef](#)]
41. Tokyo Metropolitan Government. *The Ninth Community Earthquake Risk Assessment Study*; Bureau of Urban Development, Tokyo Metropolitan Government: Tokyo, Japan, 2022.
42. Hirokawa, N.; Osaragi, T. Earthquake Disaster Simulation System: Integration of Models for Building Collapse, Road Blockage, and Fire Spread. *J. Disaster Res.* **2016**, *11*, 175–187. [[CrossRef](#)]
43. Tang, K.; Osaragi, T. Multi-Objective Evcuation Planning Model Considering Post-Earthquake Fire Spread: A Tokyo Case Study. *Sustainability* **2024**, *16*, 3989. [[CrossRef](#)]

Disclaimer/Publisher’s Note: The statements, opinions and data contained in all publications are solely those of the individual author(s) and contributor(s) and not of MDPI and/or the editor(s). MDPI and/or the editor(s) disclaim responsibility for any injury to people or property resulting from any ideas, methods, instructions or products referred to in the content.